

Matrix effect on vibrational frequencies: Experiments and simulations for HCl and HNgCl (Ng = Kr and Xe)

Jaroslav Kalinowski,¹ R. Benny Gerber,^{1,2} Markku Räsänen,¹ Antti Lignell,^{1,a)} and Leonid Khriachtchev^{1,b)}

¹Department of Chemistry, University of Helsinki, P.O. Box 55, FI-00014, Finland

²Department of Physical Chemistry, Hebrew University, Jerusalem 91904, Israel and Department of Chemistry, University of California, Irvine, California 92697, USA

(Received 5 December 2013; accepted 14 February 2014; published online 5 March 2014)

We study the environmental effect on molecules embedded in noble-gas (Ng) matrices. The experimental data on HXeCl and HKrCl in Ng matrices is enriched. As a result, the H–Xe stretching bands of HXeCl are now known in four Ng matrices (Ne, Ar, Kr, and Xe), and HKrCl is now known in Ar and Kr matrices. The order of the H–Xe stretching frequencies of HXeCl in different matrices is $\nu(\text{Ne}) < \nu(\text{Xe}) < \nu(\text{Kr}) < \nu(\text{Ar})$, which is a *non-monotonous* function of the dielectric constant, in contrast to the “classical” order observed for HCl: $\nu(\text{Xe}) < \nu(\text{Kr}) < \nu(\text{Ar}) < \nu(\text{Ne})$. The order of the H–Kr stretching frequencies of HKrCl is consistently $\nu(\text{Kr}) < \nu(\text{Ar})$. These matrix effects are analyzed theoretically by using a number of quantum chemical methods. The calculations on these molecules (HCl, HXeCl, and HKrCl) embedded in single Ng’ layer cages lead to very satisfactory results with respect to the relative matrix shifts in the case of the MP4(SDQ) method whereas the B3LYP-D and MP2 methods fail to fully reproduce these experimental results. The obtained order of frequencies is discussed in terms of the size available for the Ng hydrides in the cages, probably leading to different stresses on the embedded molecule. Taking into account vibrational anharmonicity produces a good agreement of the MP4(SDQ) frequencies of HCl and HXeCl with the experimental values in different matrices. This work also highlights a number of open questions in the field.
 © 2014 AIP Publishing LLC. [<http://dx.doi.org/10.1063/1.4866913>]

I. INTRODUCTION

Matrix IR spectroscopy was invented as a method to investigate isolated species especially those with low energetic stability and high chemical reactivity as well as chemical and photochemical reactions.^{1–3} An inert matrix and low temperature make possible to measure vibrational spectra of isolated species over an extended period of time without essential perturbation from the environment. This method is also very suitable to study intermolecular interactions, including hydrogen bonding, which are usually analyzed by comparing the IR spectra of the monomers and complexes.

From the very beginning of matrix-isolation research, it was noticed that the matrix itself can affect the properties of the embedded species. The simplest matrix effect is probably a change of vibrational frequencies of matrix-isolated species with respect to the gas-phase values. The experience of matrix-isolation research shows that the smallest shift of the vibrational bands (from the gas phase) occurs for species in a Ne matrix whereas the strongest shift is usually observed (among the practical noble gases) for Xe matrices. The classical example of this trend is reported for the stretching frequencies of hydrogen halides HY, all showing the order $\nu(\text{gas}) > \nu(\text{Ne}) > \nu(\text{Ar}) > \nu(\text{Kr}) > \nu(\text{Xe})$.⁴ These matrix-induced shifts can be qualitatively understood in terms of solvation

of a molecule in a polarizable medium. Simulations of small molecules in noble-gas (Ng) clusters lead to reasonable agreement with experimental matrix effect as, for example, for HF in Ar clusters.⁵ However, this order of stretching frequencies is not general; for example, it is not valid for the CH stretching mode of formic acid;⁶ thus, each case should be considered specifically.

Noble-gas hydrides with the formula HNgY (Ng = Ar, Kr, and Xe; Y = an electronegative fragment) are supposed to be very sensitive to external influences due to the relatively weak chemical bonding and large dipole moments.^{7–10} The complexes of noble-gas hydrides with other molecules have attracted both theoretical and experimental interest.^{9,10} Upon interaction with other molecules, the HNgY molecules as a rule exhibit blue shifts of the H–Ng stretching frequencies with a few theoretical exceptions. These blue shifts are observed not only for interaction with the H–Ng part, which may be called “improper hydrogen bond,”¹¹ but also for intermolecular interactions without bonding to the hydrogen atom of HNgY. This blue-shift effect was explained by the enhanced charge separation $(\text{HXe})^+\text{Y}^-$ upon complex formation.¹⁰

Based on the experience with the HNgY complexes,¹⁰ one may expect to observe higher H–Ng stretching frequencies in matrices with larger dielectric constants. In fact, the calculations with the polarizable continuum model predict exactly this trend.¹² This intuitive conclusion seemed to find support in experiments with HXeCl and HXeBr in Ne matrices where the H–Xe stretching frequencies were lower than

^{a)}Present address: Arthur Amos Noyes Laboratory of Chemical Physics, California Institute of Technology, 1200 East California Boulevard, Pasadena, California 91125, USA.

^{b)}E-mail: leonid.khriachtchev@helsinki.fi

those in Xe matrices (by 35 and 52 cm^{-1} , respectively).¹³ More surprisingly, HXeCl and HXeBr in a Kr matrix were reported to absorb at higher frequencies (by 15 and 20 cm^{-1}) than in a Xe matrix.¹⁴ Indeed, the lower H–Xe stretching frequency in a Ne matrix can be discussed in terms of a smaller $(\text{HXe})^+\text{Y}^-$ charge separation; however, it is unclear why solvation in a Kr matrix produces a stronger charge separation than that in a Xe matrix. More recent experiments have shown the order $\nu(\text{Ar}) > \nu(\text{Kr}) > \nu(\text{Xe}) > \nu(\text{Ne})$ for HXeBr and HXeCCH.^{12,15} All these data suggest that the matrix shift of the H–Xe stretching mode is *non-monotonous* with respect to the matrix dielectric constant; thus, our first intuitive expectation is not absolutely correct at least with respect to Ar, Kr, and Xe matrices.

To our knowledge, theoretical explanation of these experimental observations on HNgY molecules in different matrices is missing. The number of theoretical works dealing with HNgY molecules in clusters is very limited (in contrast to the 1:1 complexes). The blue-shifting effect of the matrix on the H–Ng stretching mode was first found in the calculations of Runeberg *et al.* for $\text{HArF}@\text{Ar}_6$ where a shift of +38 cm^{-1} of the H–Ar stretching mode was promoted by the interaction with the cluster.¹⁶ Matrix effects on several HNgY molecules were studied by Bihary *et al.*,¹⁷ but the used interaction potentials were not of quantitative accuracy, and the results were not satisfactory. Among other attempts, we mention the matrix-site splitting of the H–Ar stretching mode of HArF in an Ar matrix successfully simulated by Bochenkova *et al.*^{18,19} Liu *et al.* applied the polarizable continuum model to different Ng molecules to simulate matrix-solvation effects.²⁰ In particular, they obtained blue shifts of the H–Xe stretching mode of HXeCl and HXeBr as a result of solvation in a Xe matrix (+120 and +135 cm^{-1} , respectively). Tsuge *et al.* have recently used the polarizable continuum model to calculate the properties of HXeBr and HXeCCH in Ng' matrixes (Ng' = Ne, Ar, Kr, and Xe), and the order of H–Xe stretching frequencies $\nu(\text{Xe}) > \nu(\text{Kr}) > \nu(\text{Ar}) > \nu(\text{Ne})$ has been obtained for both molecules, in disagreement with the experimental results.¹² The recent B3LYP-D study by Cohen *et al.* has been focused on simulations of HXeBr in CO_2 and Xe matrices,²¹ and reasonable agreement with the experimental results has been found.

The main objective of the present work is to study the matrix effect on the vibrational spectra of embedded molecules. First, we enrich experimental spectroscopic data on HXeCl and HKrCl in Ng matrices. Second, we perform simulations of these molecules as well as of HCl in single layer cages of various noble gases Ng' optimized with the B3LYP-D, MP2, and MP4(SDQ) methods.

II. EXPERIMENT

A. Experimental details

The gaseous mixtures of HCl with different noble gases were deposited onto a cold CsI substrate in closed-cycle helium cryostats (APD, DE 202A for Ar, Kr, and Xe matrices and RDK-408D, Sumitomo Heavy Industries for a Ne matrix). The IR absorption spectra in the 4000 to 400 cm^{-1} range

were measured with a Nicolet SX60 FTIR spectrometer (resolution 1 cm^{-1}). The matrices were photolyzed with a 193-nm excimer laser (MPB, model MSX-250, pulse energy density $\sim 10 \text{ mJ cm}^{-2}$) using typically 2000 pulses at 8.5 K for Ar, Kr, and Xe matrices. Photolysis in a Ne matrix was performed with a Kr lamp (Ophos) at 4.3 K. The IR spectra were measured at the lowest operation temperatures of the cryostats.

B. Experimental results

The IR spectra of HCl in different matrices are well-known.^{4,22–25} The $R(0)$ branch produces the strongest bands at 2900, 2887.5, 2872.5, and 2858 cm^{-1} in Ne, Ar, Kr, and Xe matrices, respectively, red-shifted from the gas-phase value of 2905.7 cm^{-1} (for the main isotope ^{35}Cl). The H^{37}Cl absorptions are $\sim 2 \text{ cm}^{-1}$ lower in energy. The Q branch corresponds to relatively weak bands at 2866, 2853, and 2838 cm^{-1} in Ar, Kr, and Xe matrices, respectively, red-shifted from the gas-phase band origin at 2886 cm^{-1} .²⁶

Addition of Xe to an HCl/Ng' (Ng' = Ne and Ar in our experiments) mixture produces some amount of the $\text{HCl}\cdots\text{Xe}$ complex in the Ng' matrix. The most evident is the formation of the $\text{HCl}\cdots\text{Xe}$ complex band at 2868 cm^{-1} in a Ne matrix (2076 cm^{-1} for $\text{DCl}\cdots\text{Xe}$). It is interesting to estimate the shift of the HCl band upon complexation with a Xe atom. This shift should be calculated with respect to the Q branch, which unfortunately has not been observed in a Ne matrix. However, we can estimate its position by using the spectrum in an Ar matrix and assuming a similar matrix effect on the R and Q branches. As a result, we obtain the Q branch at about 2879 cm^{-1} for HCl in a Ne matrix. It follows that interaction with a Xe atom changes the HCl frequency in a Ne matrix by -11 cm^{-1} . More detailed description of IR spectroscopy of HCl species exceeds the scope of the present work.

We performed experiments with a mixture of Xe, HCl, and DCl in a Ne matrix. UV photolysis dissociates HCl and DCl. H(D) atoms have the highest probability to escape the cage and they are isolated in the matrix.²⁷ In this case, some amount of $\text{Cl}\cdots\text{Xe}$ pairs is expected to be stabilized in the matrix. Thermally mobilized H(D) atoms can react with these $\text{Cl}\cdots\text{Xe}$ pairs to produce HXeCl and DXeCl molecules. It is interesting that the corresponding bands appear already after photolysis (prior to annealing), which indicates the locality of photolysis of HCl in a Ne matrix (spectrum a in Figure 1). Similar light-induced formation has been reported for a number of other HNgY molecules in Ar, Kr, and Xe matrices.^{28–31} Annealing of the matrix enhances the amount of HXeCl and DXeCl, as typical for this preparation method (spectrum b in Figure 1). The HNgY molecules can be easily decomposed by UV light, which is their characteristic feature, and the HXeCl band in a Ne matrix behaves accordingly (spectrum c in Figure 1).

The bands of HXeCl and DXeCl in a Ne matrix are at 1612 and 1173 cm^{-1} , which is in good agreement with the data reported by Lorenz *et al.*¹³ The reason to repeat the experiments by Lorenz *et al.* is that their cryostat had the lowest temperature of 8 K, which is somewhat too high to work with Ne matrices; however, their results are confirmed. The

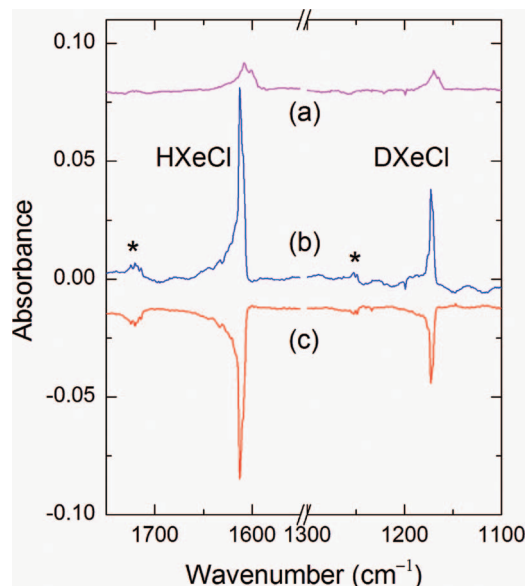


FIG. 1. HXeCl and DXeCl in a neon matrix. Shown are difference spectra presenting the results of (a) photolysis of a HCl/DCl/Xe/Ne (1/1/8/4000) matrix by a Kr lamp; (b) annealing of the photolyzed matrix for 7 min at 12 K; and (c) additional irradiation of the annealed matrix at 193 nm. The background spectra were measured before photolysis, annealing, and additional irradiation, respectively. The bands of the HXeCl⋯HCl complex and its deuterated analogue are marked by asterisks. The spectra were measured at 4.3 K.

ratio of the H–Xe and D–Xe stretching frequencies (1.374) is very similar to that measured in a Xe matrix (1.376).¹⁴ In fact, the observed small difference in the H/D frequency ratios is remarkable because it features a decrease of anharmonicity of the H–Xe stretching vibration in a Xe matrix, i.e., the strengthening of chemical bonding of HXeCl upon solvation in a Xe matrix.

In addition to the main bands at 1612 and 1173 cm^{-1} , weaker bands appear at about 1720 and 1251 cm^{-1} . These bands are observed only when HCl(DCl) and Xe are present in a Ne matrix, grow upon annealing, and they are bleached by UV light synchronously with the main HXeCl and DXeCl bands. We assign the 1720 cm^{-1} band to the HXeCl⋯HCl complex in a Ne matrix (1251 cm^{-1} for the deuterated analogues). The shifts of the H(D)–Xe stretching mode of these complexes from the corresponding monomers are about +108 and +78 cm^{-1} , respectively. Several structures of the HXeCl⋯HCl complex have been suggested by theory and observed experimentally.²⁵ The bands found in the present study presumably originate from the lowest-energy structure (calculated shift +116.7 cm^{-1}), in which the H atom of HCl interacts with the Cl atom of HXeCl. The HXeCl⋯HCl complex was previously identified in a Xe matrix, and the lowest-energy structure had two bands with shifts of +106.4 and +115.5 cm^{-1} .²⁵ Thus, the present results are in excellent agreement with the previous calculations and measurements in a Xe matrix.

Photolysis and annealing of an HCl/Xe/Ar matrix lead to the appearance of a band at 1675 cm^{-1} . This band rises at temperature of about 20 K, which is similar to the formation of HArF in an Ar matrix.²⁸ It appears only when both HCl and Xe are present in an Ar matrix and it can be easily bleached

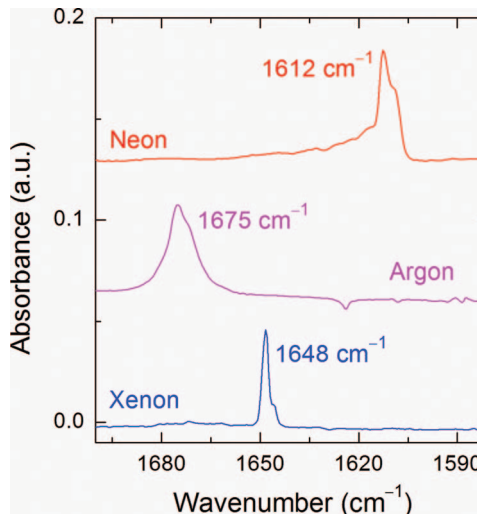


FIG. 2. HXeCl in Ne, Ar, and Xe matrices. Shown are difference spectra presenting the results of annealing of photolyzed HCl/Xe/Ne matrices (Ng = Ne, Ar, and Xe). The annealing temperatures are 12, 20, and 40 K for Ne, Ar, and Xe matrices, respectively. The background spectra were measured before annealing. The spectra are scaled for better presentation. The spectra were measured at 4.3 K for a Ne matrix and at 8.5 K for Ar and Xe matrices.

by UV light. Thus, this band can be safely assigned to HXeCl in an Ar matrix. Figure 2 shows the H–Xe stretching bands of HXeCl in Ne, Ar, and Xe matrices, located at 1612, 1675, and 1648 cm^{-1} . The H–Xe stretching frequency of HXeCl in a Kr matrix was reported previously to be 1664 cm^{-1} .¹⁴ Thus, the following order of the H–Xe stretching frequencies $\nu(\text{Ar}) > \nu(\text{Kr}) > \nu(\text{Xe}) > \nu(\text{Ne})$ is obtained for HXeCl in different matrices. The same order of frequencies has also been found for HXeBr and HXeCCH.^{12,15} It should be mentioned that the efficiency of the formation of HXeCl in different matrices strongly depends on the experimental conditions. However, it seems that the amount of HXeCl in Ne and Ar matrices is comparable with that in a Xe matrix. As another interesting observation, the HXeCl band is much broader in an Ar matrix than that in a Xe matrix, which may be connected with more regular environment in the latter case.

We expand these experiments on Ng hydrides in “foreign” matrices to the case of HKrCl, for the first time for a Kr-containing molecule. Photolysis and annealing of HCl/Kr/Ar matrix produce a band at 1482.5 cm^{-1} (Figure 3). This band rises at temperature of about 20 K, which is similar to the formation of HArF.²⁸ This band appears only when both HCl and Kr are present in an Ar matrix and it can be easily decomposed by UV light; thus, it can be safely assigned to HKrCl in an Ar matrix. This band is blue-shifted from the HKrCl band in a Kr matrix by +6.5 cm^{-1} (Figure 3). This observation shows the $\nu(\text{Ar}) > \nu(\text{Kr})$ order for the H–Kr stretching band of HKrCl, i.e., the same as for HXeCl, HXeBr, and HXeCCH. The formation of HKrCl in an Ar matrix is inefficient compared to a Kr matrix (the lower spectrum in Figure 3 is multiplied by 60). Our attempts to prepare HKrCl in a neon matrix have failed, which can be connected with the intrinsic instability of HKrCl or a relatively high formation barrier.

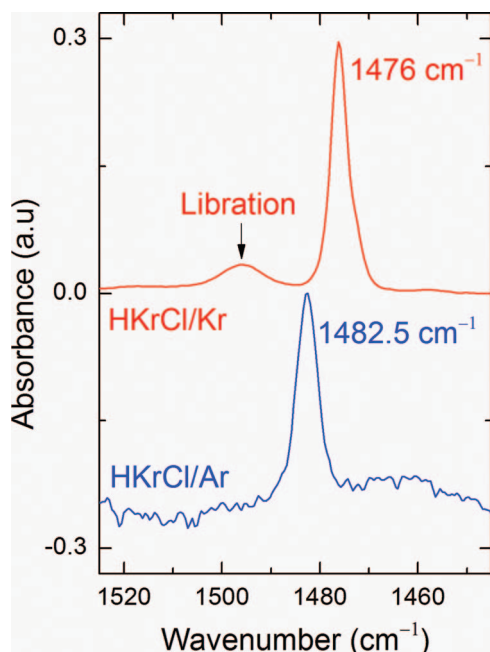


FIG. 3. HKrCl in Ar and Kr matrices. Shown are difference spectra presenting the results of annealing of photolyzed HCl/Kr/Ng matrices (Ng = Ar and Kr). The annealing temperatures are 20 and 30 K for Ar and Kr matrices, respectively. The background spectra were measured before annealing. The librational band of HKrCl in a Kr matrix is marked.⁵⁴ The spectra are scaled for better presentation. The spectra were measured at 8.5 K.

III. QUANTUM CHEMICAL CALCULATIONS

A. Computational details

The calculations were mainly performed with the B3LYP-D,^{32–34} MP2,³⁵ and MP4(SDQ)³⁵ methods. In addition to these methods, the 1:1 complexes were calculated with the CCSD(T) method.³⁶ All calculations were done with Dunning's aug-cc-pVTZ basis set to avoid large basis-set superposition errors.^{37–39} Pseudopotentials, supplied with the aug-cc-pVTZ basis set, were used for Kr and Xe atoms. The B3LYP-D, MP2, and CCSD(T) calculations were performed using the GAMESS package.⁴⁰

The MP4 method is not widely used nowadays; however, it is sometimes employed to optimize the geometry of hydrocarbons and organic molecules.^{41,42} This level of theory is unusual to calculate IR frequencies because of its high computational cost. In the hybrid MP2/MP4 approach recently proposed by us, the MP4(SDQ) potential has been used to improve the anharmonic MP2 frequencies of organic molecules.⁴³ The MP4 correlation energy correction consists of the MP2, MP3(D), MP4(SDQ), and MP4(T) corrections, which is known to describe well the dispersion interactions.^{44,45} While the MP2 method scales as nN^4 where n is the number of the occupied and correlated molecular orbitals and N is the total number of the basis functions, the third-order correction (MP3(D)) scales as n^2N^4 and the fourth-order correction with single, double, and quadruple substitutions (MP4(SDQ)) scales as n^3N^3 . Because the scaling of MP4(T) is n^3N^4 , the energy calculations with MP4(SDQ) are much faster than with MP4(SDTQ). While the MP4(SDQ) method can strongly underestimate attractive

dispersion forces,^{46,47} MP2 is known to overestimate dispersion interactions.^{48,49} In this work, we will show that the MP4(SDQ) potential can offer great advantages over MP2 for systems dominated by dispersion forces.

For all MP4 calculations, we used a code recently developed by us.⁴⁹ The MP4(SDQ) energies can be evaluated directly from atomic integrals, in the spirit of the direct Hartree-Fock method.⁵⁰ However, in the present work, the calculation was done using a parallelized algorithm where the integrals are kept in memory distributed over the available CPUs. This approach avoids the bottleneck of the data transfer from the hard disk. The used massively parallelized algorithm is found to be very efficient for the calculations reported here.

Using the MP4(SDQ) method, we also calculated anharmonic frequencies of HXeCl, HKrCl, and HCl molecules in single Ng' layers. The supramolecular system is too large for the full Vibrational Self-Consistent Field (VSCF) calculations taking into account the mode couplings. Instead, we limited the calculation to the diagonal approximation. First, the potentials along each normal coordinate, with the other modes in the equilibrium, were computed. Then, the anharmonic frequencies were calculated for each mode by numerical solution of the one-dimensional Schrödinger equation. This approach represents the first step in the VSCF algorithms.^{51–53} It neglects the coupling between different vibrational modes and includes only the intrinsic anharmonicity of the normal modes.

An important feature of the *ab initio* vibrational methods used here is that all interactions in the system are treated on the same footing, i.e., using the MP4(SDQ) quantum chemical potential. In particular, no pairwise interaction approximation is made between the Ng' atoms or between the Ng' atoms and HNgCl.

B. 1:1 complexes

The Ng'⋯HNgY complex is the first approximation of the Ng' matrix effect on the HNgY molecule. This single Ng' atom already produces a large change in the H–Ng stretching frequency. The different complex structures give the general idea about possible interactions between the HNgY molecule and matrix atoms.⁵⁴ The lowest energy 1:1 complexes Ng'⋯HKrCl (Ng' = Ar and Kr) and Ng'⋯HXeCl (Ng' = Ne, Ar, Kr, and Xe) have the structure where the Ng' atom interacts with the hydrogen atom. The Ng' atom does not influence much the HNgY geometry, changing the bond lengths by less than 0.01 Å. The CCSD(T) method predicts the linear geometry of these complexes. According to other methods, the structures are slightly bent with the Ng'–H–Ng angle from 179.0° to 179.5°. The only exception is the absolutely linear Ne⋯HXeCl complex at the MP4(SDQ) level of theory.

The harmonic H–Ng stretching frequencies seem to be highly overestimated by all methods (Table I), which is typical for harmonic calculations of HNgY molecules.⁷ More importantly for the present study, the order of frequencies obtained for the 1:1 complexes mismatches the experimental frequencies in matrices. In fact, the MP2, MP4(SDQ), and CCSD(T) methods predict the highest frequency for the

TABLE I. Calculated harmonic H–Ng stretching frequencies (in cm^{-1}) for isolated HNgCl species and the 1:1 Ng'...HNgCl complexes.^a

	B3LYP-D	MP2	MP4(SDQ)	CCSD(T)
HKrCl	1761	1926	1936	1663
Ar...HKrCl	1791[+30]	2036 [+110]	2023 [+87]	1776 [+113]
Kr...HKrCl	1813[+52]	2046 [+120]	2049 [+113]	1821 [+158]
HXeCl	1756	1932	1915	1780
Ne...HXeCl	1755 [−1]	1966 [+34]	1940 [+25]	1809 [+29]
Ar...HXeCl	1753 [−3]	1981 [+49]	1953 [+38]	1827 [+47]
Kr...HXeCl	1729 [−27]	1995 [+63]	1966 [+51]	1848 [+68]
Xe...HXeCl	1686 [−70]	1966 [+34]	1956 [+41]	1833 [+53]

^aShifts from the isolated molecule are given in brackets.

complexes with Kr. Unexpectedly large blue shifts are obtained for the Ne...HXeCl complex with the MP2, MP4(SDQ), and CCSD(T) methods. Indeed, the effect of Ne is usually expected to be quite small. There are doubts about the description of the Ng'...HXeCl complex by the B3LYP-D method because of the red shifts obtained with respect to vacuum and sharp disagreement with other methods. In general, it follows that the approximation of the 1:1 complexes does not explain the experimental results obtained in matrices. Clearly, more noble-gas atoms are needed to reproduce the matrix effect. The same conclusion was derived earlier by Tanskanen *et al.* in their study of HXeCCH in Ar, Kr, and Xe matrices.¹⁵

The lowest energy Ng'...HCl complexes have a linear geometry where the Ng atom interacts with the H atom. These 1:1 complexes calculated by all four methods are linear with the $C_{\infty v}$ symmetry. The harmonic vibrational frequencies of the Ng'...HCl complexes are shown in Table II. Interaction with Ne unexpectedly produces a blue shift on the HCl frequency by all methods. The MP2, MP4(SDQ), and CCSD(T) methods lead to intuitively correct order of frequencies where the frequency decreases when the Ng' polarizability increases. The B3LYP-D results feature a different order for the complexes with Ar and Kr. The calculations for the Xe...HCl complex give red shifts that are substantially larger than found experimentally for this complex in a Ne matrix (-11 cm^{-1}).

C. Single-layer model

The next step to describe the matrix effect is a single-layer model. In this model, HNgY is surrounded by a layer of Ng' atoms. We construct the layer adding additional Ng' atoms to the system one by one starting from the most

TABLE II. Calculated harmonic HCl vibrational frequencies (in cm^{-1}) for isolated HCl and the Ng'...HCl complexes.^a

	B3LYP-D	MP2	MP4(SDQ)	CCSD(T)
HCl	2940	3057	3033	3004
Ne...HCl	2948 [+8]	3078 [+21]	3046 [+13]	3017 [+13]
Ar...HCl	2937 [−3]	3065 [+8]	3038 [+5]	3007 [+3]
Kr...HCl	2938 [−2]	3058 [+1]	3026 [−7]	2995 [−9]
Xe...HCl	2905 [−35]	3038 [−19]	3012 [−21]	2976 [−28]

^aShifts from the isolated molecule are given in brackets.

stable 1:1 complex and optimizing the layer at each step until it becomes complete. The complete layer is optimized as a global minimum for distribution of Ng' atoms around the molecule and mimics the matrix cage. Two criteria are used for the completion of the layer. First, the cage is considered complete when an additional noble-gas atom is clearly outside the first shell. Second, this additional atom shifts the H–Ng stretching frequency by less than 0.2 cm^{-1} whereas an addition of an atom in the first shell shifts the H–Ng stretching frequency by a much larger value. The cage seems to have very small effect on the geometry of the HNgY molecules. The H–Ng and Ng–Y bond lengths change by less than 0.01 and 0.02 Å, respectively, and the HNgY molecules remain linear inside the cages. For all computational methods, the Ar, Kr, and Xe cages contain the same number of atoms, 17 and 12 for HNgCl and HCl, respectively. The Ne cages in all studied cases consist of 22 and 17 atoms for HNgCl and HCl molecules, respectively.

In the Ar, Kr, and Xe cages, one of the cage atoms forms the perfectly linear Ng'...HNgCl and Ng'...HCl geometries following the motifs obtained for the 1:1 complexes. With respect to the corresponding axis, the Ar, Kr, and Xe cages have the C_{5v} symmetry (Figure 4). The Ne cages have in most cases the C_1 symmetry (Figure 5). The only exception here is the Ne cage for HXeCl calculated by the MP2 method where one of the Ne cage atoms forms the linear Ne...HXeCl geometry and the cage has the C_{5v} symmetry. The structure of the simulated single layer cages considerably differs from that of the corresponding Ng crystals. As compared with a single substitutional site in an Ng crystal, the single layer cages are strongly distorted along the HNgCl axis which elongates the cage. This large distortion is at least partially a result of including only single layer in the simulation. In all cases, the level of distortion is even higher if the single layer cages are compared with double substitutional sites of the Ng crystals.

In the optimized systems, the cages embedding HNgCl can be either stretched or compressed. To address this issue we compared the average Ng–Ng distance in calculated cages with the experimental Ng–Ng distances in the corresponding crystals (Table SI of the supplementary material).⁵⁵

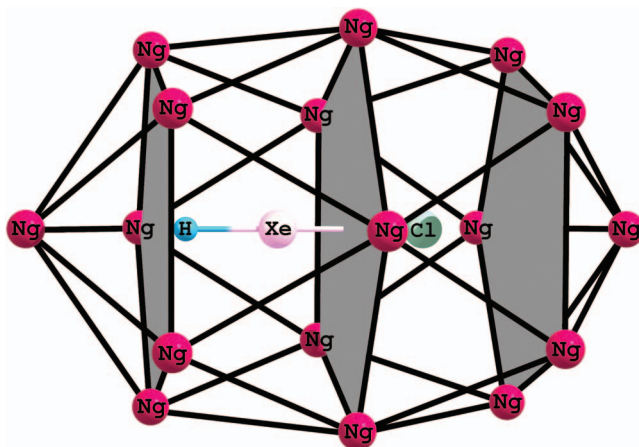


FIG. 4. HXeCl embedded in Ar, Kr, and Xe cages. The case of HKrCl in Ar and Kr cages is very similar.

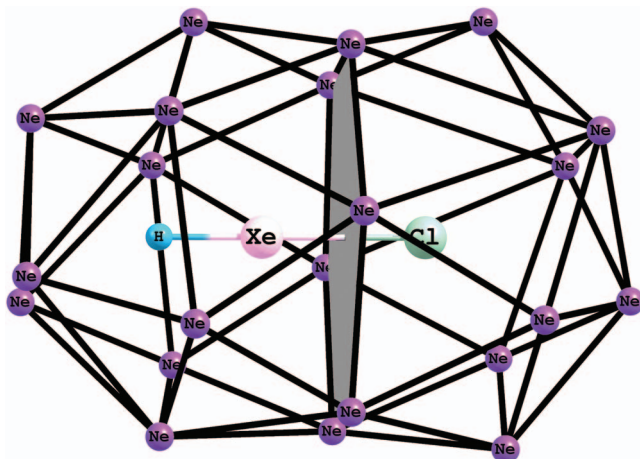


FIG. 5. HXeCl embedded in a Ne cage.

The results are shown in Table III. For example, the Xe cage calculated by the B3LYP-D and MP2 methods is compressed with respect to the equilibrium whereas it is slightly stretched in the case of the MP4(SDQ) method. The normalized average distances gradually increase for Kr, Ar, and Ne, with an exception of the case of Ne and MP4(SDQ).

Table IV presents the harmonic frequencies of HKrCl and HXeCl molecules in the single layer cages. For HKrCl, all three methods reproduce well the experimental order $\nu(\text{Kr}) < \nu(\text{Ar})$ and the corresponding frequency difference (6.5 cm^{-1}). For HXeCl, the MP4(SDQ) method reproduces correctly the order of the experimental frequencies $\nu(\text{Ne}) < \nu(\text{Xe}) < \nu(\text{Kr}) < \nu(\text{Ar})$ and the frequency differences. In contrast, the B3LYP-D method does not describe the frequency order between Ar and Kr matrices. The MP2 results are even less satisfactory because the red shift of the frequency is predicted for the heavier noble gases with respect to Ne, which contradicts the experiment.

It is interesting to compare the calculated H–Ng stretching frequencies of HKrCl and HXeCl in vacuum, 1:1 complexes, and single-layer cages (Table SII of the supplementary material).⁵⁵ In the B3LYP-D calculations, the insertion of the molecule into the cage increases the H–Ng stretching

TABLE III. Normalized distances in single Ng' layer cages for HNgCl and HCl molecules.^a

	Ng	B3LYP-D	MP2	MP4(SDQ)
HKrCl	Ar	1.081	0.976	1.051
	Kr	1.001	0.955	1.003
HXeCl	Ne	1.118	1.076	0.987
	Ar	1.108	0.997	1.082
	Kr	1.017	0.969	1.013
	Xe	0.927	0.880	1.002
HCl	Ne	1.099	1.033	0.962
	Ar	1.054	0.954	1.003
	Kr	0.978	0.935	0.956
	Xe	0.920	0.885	0.973

^aValues are the average Ng'–Ng' distances in a given cage normalized by the Ng'–Ng' distance in the corresponding noble-gas crystal (see Table SI of the supplementary material).⁵⁵ The standard deviations are in all cases lower than 0.02.

TABLE IV. Calculated harmonic H–Ng stretching frequencies (in cm^{-1}) of HNgY in single Ng' layer cages and the experimental frequencies in different matrices.^a

	B3LYP-D	MP2	MP4(SDQ)	Experiment
HKrCl	1761 [–91]	1926 [–64]	1936 [+84]	...
HKrCl @Ar	1852	1990	1852	1483
HKrCl @Kr	1845 [–7]	1984 [–6]	1846 [–6]	1476 [–7]
HXeCl	1756 [–61]	1932 [–34]	1915 [+50]	...
HXeCl @Ne	1817	1966	1865	1612
HXeCl @Ar	1840 [+23]	1963 [–3]	1910 [+46]	1675 [+63]
HXeCl @Kr	1852 [+35]	1952 [–14]	1899 [+34]	1664 [+52]
HXeCl @Xe	1825 [+8]	1920 [–46]	1880 [+15]	1648 [+36]

^aShifts from the lightest noble gas (Ar for HKrCl and Ne for HXeCl) are given in brackets.

frequency as compared to vacuum and to the 1:1 complexes with the same Ng' atom. For the MP2 method, the cage also increases the frequency with respect to vacuum (with exception of HXeCl in Xe) but decreases it with respect to the 1:1 complexes. In the case of MP4(SDQ), the frequencies obtained in the cages are always smaller than the frequencies in vacuum and the 1:1 complexes. The H–Ng stretching frequency can be considered as a measure of the stability of HNgY molecules with respect to the three-body (H + Ng + Y) dissociation channel. Thus, the MP4(SDQ) method seems to predict that the Ng' layers destabilize the HNgCl molecules, which is in sharp contradiction with the prediction of the polarizable continuum model.^{12,20} The first Ng' atom that forms the 1:1 complex with the HNgY molecule seems to stabilize the molecule, but the rest of the layer destabilizes HNgY consistently according to all methods excepting B3LYP-D. In fact, in computational studies of HHeF in Xe clusters, the H–He stretching frequency was maximum in the 1:1 complex and decreased for larger Xe clusters.⁵⁶

The results for HCl in the single-layer cages are shown in Table V. Interaction with Ne is reasonably described by B3LYP-D featuring a minor shift (the experimental frequency difference between the gas phase and a Ne matrix is -6 cm^{-1}). The MP2 and MP4(SDQ) calculations overestimate the Ne matrix effect, predicting shifts of -28 and -47 cm^{-1} . On the other hand, all three methods reproduce well the experimental shifts by heavier Ng' matrices with respect to Ne. With respect to the 1:1 complexes and vacuum, the single layers decrease the HCl vibrational frequency (Table SIII of the supplementary material).⁵⁵

Tables VI and VII show the results of the anharmonic calculations on HNgCl and HCl in different Ng' layers performed with the MP4(SDQ) methods. It is seen that the accounting for anharmonicity produces no qualitative changes in the shifts between the matrices. On the other hand, the absolute frequencies change significantly (decrease with respect to the harmonic approximation) and the calculated values are in a good agreement with the experimental results. For example, the theoretical and experimental H–Xe stretching frequencies for HXeCl in the Xe environment are 1650 and 1648 cm^{-1} , respectively. The gas-phase values of the HCl frequencies are 2883 cm^{-1} (theory) and 2886 cm^{-1} (experiment). For HCl in the Xe surrounding, we have 2820 cm^{-1}

TABLE V. Calculated harmonic vibrational frequencies for HCl in single Ng' layer cages and the experimental frequencies in the gas phase and different matrices (in cm^{-1}).^a

	B3LYP-D	MP2	MP4(SDQ)	Experiment	
				<i>Q</i> branch	<i>R</i> (0) branch
HCl	2940 [0]	3057 [+28]	3033 [+47]	2886 ^b [+7]	2905 [+5]
HCl@Ne	2940	3029	2986	2879 ^c	2900
HCl@Ar	2931 [−9]	3017 [−12]	2975 [−11]	2866 [−13]	2887 [−13]
HCl@Kr	2916 [−24]	2997 [−32]	2961 [−25]	2853[−26]	2872 [−28]
HCl@Xe	2894 [−46]	2973 [−56]	2937 [−49]	2838 [−49]	2852 [−48]

^aShifts from the Ne case are given in brackets.^bBand origin.^cEstimate.

(theory) and 2838 cm^{-1} (experiment). For HKrCl, the agreement is worse, for example, the theoretical and experimental frequencies (in the Kr environment) are 1582 and 1476 cm^{-1} whereas the experimental shift to the Ar surrounding is reproduced well. It seems that the MP4(SDQ) calculations overestimate chemical bonding of HKrCl. The prediction for the frequencies of the HKrCl and HXeCl molecules in the gas phase are 1768 and 1812 cm^{-1} , respectively.

The relative success of MP4 over MP2 and DFT-D is most likely a result of a better description of dispersion interactions. The MP2 method is known to strongly overestimate dispersion-based interactions and Grimme's semiempirical dispersion correction, successfully used in DFT calculations, seems to have relatively low accuracy in the case of systems dominated by dispersion-like noble-gas environments.

IV. CONCLUDING DISCUSSION

In the present work, we have investigated both experimentally and theoretically the matrix effect on the vibrational properties of embedded molecules, with emphasis on Ng hydrides HKrCl and HXeCl. In the experiments, we have enriched the spectroscopic data on these species in Ng matrices, in particular, reporting for the first time the absorption bands of HKrCl and HXeCl in an Ar matrix. As a result, the H–Xe stretching bands of HXeCl are now known in four Ng matrices (from neon to xenon). HKrCl is now reported in Ar and Kr matrices. In contrast to HXeCl, the attempts to prepare HKrCl in a Ne matrix have failed, and reasons of this negative result

TABLE VI. Anharmonic frequencies (cm^{-1}) of HKrCl and HXeCl in single Ng' layer cages and the experimental values.^a

	MP4(SDQ)	Experiment
HKrCl	1768 [+175]	...
HKrCl@Ar	1593	1483
HKrCl@Kr	1582 [−11]	1476 [−7]
HXeCl	1812 [+192]	...
HXeCl@Ne	1620	1612
HXeCl@Ar	1665 [+45]	1675 [+63]
HXeCl@Kr	1651 [+31]	1664 [+52]
HXeCl@Xe	1650 [+30]	1648 [+36]

^aShifts from the lightest noble gas (Ar for HKrCl and Ne for HXeCl) are given in brackets.

may be a lack of stability of HKrCl in a Ne matrix and/or a relatively high formation barrier.

Based on the new and earlier experimental results, the environmental effect is analyzed theoretically by using several computational methods. The 1:1 complexes ($\text{Ng}'\cdots\text{HY}$ and $\text{Ng}'\cdots\text{HNgY}$) do not describe the experimental situation in matrices, as it was concluded previously.¹⁵ The MP4(SDQ) calculations of these molecules embedded in a single Ng' layers lead to satisfactory results with respect to the matrix shifts. Moreover, taking into account vibrational anharmonicity leads to good agreement of the calculated frequencies of HCl and HXeCl with the experimental values. The agreement of the absolute values is worse for HKrCl, which can be connected with very weak chemical bonding of this molecule. Indeed, the experiments may show intrinsic instability of this molecule.

The order of the H–Xe stretching frequencies $\nu(\text{Ne}) < \nu(\text{Xe}) < \nu(\text{Kr}) < \nu(\text{Ar})$ seems to be general for Ng hydrides, especially taking into account the most recent experiments on HXeBr and HXeCCH.^{12,15} It should be emphasized that the H–Xe stretching frequency of HNgY is not a monotonous function of the matrix dielectric constant. Thus, this trend follows the expectations derived from the polarizable continuum model only for the Ne environment with respect to the heavier noble gases whereas the situation with Ar, Kr, and Xe is more complicated. The present calculations suggest a possible explanation for this puzzle. We can speculate that the reason is in different stress states of the molecules in the cages. The Ar cage is significantly stretched by the presence of HNgCl hence the compressive stress appears on the

TABLE VII. Anharmonic frequencies (cm^{-1}) of HCl in single Ng' layer cages and the experimental values.^a

	MP4(SDQ)	Experiment	
		<i>Q</i> branch	<i>R</i> (0) branch
HCl	2883	2886 ^b	2905
HCl@Ne	2880 [−3]	2879 ^c [−7]	2900 [−5]
HCl@Ar	2862 [−21]	2866 [−20]	2887 [−18]
HCl@Kr	2843 [−40]	2853 [−33]	2872 [−33]
HCl@Xe	2820 [−63]	2838 [−48]	2852 [−53]

^aShifts from the molecule in vacuum are given in brackets.^bBand origin.^cEstimate.

embedded molecule. In other words, the Ar cage would be too tight for the embedded molecule whereas the Xe cage is more relaxed and the effect of stress is smaller (or even opposite). It is probable that this difference of the cage sizes is responsible for the unexpected order of the H–Xe stretching frequencies of HXeCl in Ar, Kr, and Xe matrices. The same is applicable to HKrCl in Ar and Kr environments. No experimental information on the pressure effect on HNgY molecules is available. In fact, this experiment is realistic; unfortunately, spectroscopic measurements at elevated pressures are not available in our laboratory. It is reasonable to suspect that an additional repulsive force that comes from compressive stress between the cage and HNgY molecule does not change HNgY geometry significantly but makes HNgY \rightarrow H + Ng + Cl dissociation curve steeper hence increasing the H–Ng stretching frequency.

A very unexpected result of these calculations is a large red shift obtained by the MP4(SDQ) method for the H–Ng stretching mode of HNgCl in a single Ne layer with respect to vacuum (-50 cm^{-1} for HXeCl in the harmonic approximation). This red shift strongly increases in the anharmonic calculations. For MP4(SDQ), the H–Ng stretching frequencies in all Ng' layers are smaller than in the case of vacuum. This MP4(SDQ) result is in general disagreement with other methods (B3LYP-D and MP2) and with the polarizable continuum model that predict the stabilization of Ng hydrides by the polarizable medium.^{12,20} This striking question about the validity of these MP4(SDQ) predictions will remain open until the experiments in the gas phase are performed. Another important question is how adequate the description of a solid matrix by a single layer is. Indeed, the single layer possesses no properly coordinated matrix atoms. However, calculations of larger systems with these computational methods are impossible at the present time.

ACKNOWLEDGMENTS

CSC–IT Center for Science Computing Ltd. (Espoo, Finland) is thanked for computational resources.

- ¹E. Whittle, D. A. Dows, and G. C. Pimentel, *J. Chem. Phys.* **22**, 1943 (1954).
- ²*Chemistry and Physics of Matrix-Isolated Species*, edited by L. Andrews and M. Moskovits (North Holland, Amsterdam, 1989).
- ³*Physics and Chemistry at Low Temperatures*, edited by L. Khriachtchev (Pan Stanford Publishing Pte. Ltd, Singapore, 2011).
- ⁴A. J. Barnes, H. E. Hallam, and G. F. Schimsha, *Trans. Faraday Soc.* **65**, 3159 (1969).
- ⁵A. V. Bochenkova, M. A. Suhm, A. A. Granovsky, and A. V. Nemukhin, *J. Chem. Phys.* **120**, 3732 (2004).
- ⁶A. Domanskaya, K. Marushkevich, L. Khriachtchev, and M. Räsänen, *J. Chem. Phys.* **130**, 154509 (2009).
- ⁷L. Khriachtchev, M. Räsänen, and R. B. Gerber, *Acc. Chem. Res.* **42**, 183 (2009).
- ⁸R. B. Gerber, E. Tsivion, L. Khriachtchev, and M. Räsänen, *Chem. Phys. Lett.* **545**, 1 (2012).
- ⁹S. A. C. McDowell, *Curr. Org. Chem.* **10**, 791 (2006).
- ¹⁰A. Lignell and L. Khriachtchev, *J. Mol. Struct.* **889**, 1 (2008).
- ¹¹P. Hobza and Z. Havlas, *Chem. Rev.* **100**, 4253 (2000).
- ¹²M. Tsuge, A. Lignell, M. Räsänen, and L. Khriachtchev, *J. Chem. Phys.* **139**, 204303 (2013).
- ¹³M. Lorenz, M. Räsänen, and V. E. Bondybey, *J. Phys. Chem. A* **104**, 3770 (2000).

- ¹⁴M. Pettersson, J. Lundell, and M. Räsänen, *J. Chem. Phys.* **102**, 6423 (1995).
- ¹⁵H. Tanskanen, L. Khriachtchev, J. Lundell, and M. Räsänen, *J. Chem. Phys.* **125**, 074501 (2006).
- ¹⁶N. Runeberg, M. Pettersson, L. Khriachtchev, J. Lundell, and M. Räsänen, *J. Chem. Phys.* **114**, 836 (2001).
- ¹⁷Z. Bihary, G. M. Chaban, and R. B. Gerber, *J. Chem. Phys.* **116**, 5521 (2002).
- ¹⁸A. V. Bochenkova, D. A. Firsov, and A. V. Nemukhin, *Chem. Phys. Lett.* **405**, 165 (2005).
- ¹⁹A. V. Bochenkova, V. E. Bochenkov, and L. Khriachtchev, *J. Phys. Chem. A* **113**, 7654 (2009).
- ²⁰G. Liu, Y. Zhang, Z. Wang, Y. Wang, X. Zhang, and W. Zhang, *Comput. Theor. Chem.* **993**, 118 (2012).
- ²¹A. Cohen, M. Tsuge, L. Khriachtchev, M. Räsänen, and R. B. Gerber, *Chem. Phys. Lett.* **594**, 18 (2014).
- ²²M. T. Bowers and W. H. Flygare, *J. Chem. Phys.* **44**, 1389 (1966).
- ²³D. E. Mann, N. Acquista, and D. White, *J. Chem. Phys.* **44**, 3453 (1966).
- ²⁴A. Lignell, L. Khriachtchev, M. Pettersson, and M. Räsänen, *J. Chem. Phys.* **118**, 11120 (2003).
- ²⁵A. Lignell, J. Lundell, L. Khriachtchev, and M. Räsänen, *J. Phys. Chem. A* **112**, 5486 (2008).
- ²⁶D. H. Rank, W. B. Birtley, D. P. Eastman, B. S. Rao, and T. A. Wiggings, *J. Opt. Soc. Am.* **50**, 1275 (1960).
- ²⁷V. A. Apkarian and N. Schwentner, *Chem. Rev.* **99**, 1481 (1999).
- ²⁸L. Khriachtchev, M. Pettersson, N. Runeberg, J. Lundell, and M. Räsänen, *Nature (London)* **406**, 874 (2000).
- ²⁹M. Pettersson, L. Khriachtchev, J. Lundell, S. Jolkkonen, and M. Räsänen, *J. Phys. Chem. A* **104**, 3579 (2000).
- ³⁰L. Khriachtchev, M. Pettersson, J. Lundell, and M. Räsänen, *J. Chem. Phys.* **114**, 7727 (2001).
- ³¹L. Khriachtchev, S. Tapio, M. Räsänen, A. Domanskaya, and A. Lignell, *J. Chem. Phys.* **133**, 084309 (2010).
- ³²A. D. Becke, *J. Chem. Phys.* **98**, 5648 (1993).
- ³³P. J. Stephens, J. F. Devlin, C. F. Chabalowski, and M. J. Frisch, *J. Phys. Chem.* **98**, 11623 (1994).
- ³⁴S. Grimme, J. Antony, S. Ehrlich, and H. Krieg, *J. Chem. Phys.* **132**, 154104 (2010).
- ³⁵C. Møller and M. S. Plesset, *Phys. Rev. Lett.* **46**, 618 (1934).
- ³⁶G. E. Scuseria, C. L. Janssen, and H. F. Schaefer, *J. Chem. Phys.* **89**, 7382 (1988).
- ³⁷T. H. Dunning, Jr., *J. Chem. Phys.* **90**, 1007 (1989).
- ³⁸D. E. Woon and T. H. Dunning, Jr., *J. Chem. Phys.* **98**, 1358 (1993).
- ³⁹K. A. Peterson, D. Figgen, E. Goll, H. Stoll, and M. Dolg, *J. Chem. Phys.* **119**, 11113 (2003).
- ⁴⁰M. S. Gordon and M. W. Schmidt, in *Theory and Applications of Computational Chemistry, the First Forty Years*, edited by C. Dykstra, G. Frenking, K. Kim, and G. Scuseria (Elsevier Science, 2005), pp. 1167–1189.
- ⁴¹A. A. Al-Saadi, *J. Mol. Struct.* **1023**, 115 (2012).
- ⁴²H. M. Badawi, *Spectrochim. Acta A* **82**, 63 (2011).
- ⁴³J. F. Dobson, K. McLennan, A. Rubio, J. Wang, T. Gould, H. M. Le, and B. P. Dinte, *Aust. J. Chem.* **54**, 513 (2001).
- ⁴⁴R. M. Balabin, *Chem. Phys.* **352**, 267 (2008).
- ⁴⁵S. Tsuzuki, T. Uchimaru, and K. Tanabe, *Chem. Phys. Lett.* **287**, 202 (1998).
- ⁴⁶S. Tsuzuki, T. Uchimaru, K. Matsumura, M. Mikami, and K. Tanabe, *Chem. Phys. Lett.* **319**, 547 (2000).
- ⁴⁷R. Podeszwa, *J. Phys. Chem. A* **112**, 8884 (2008).
- ⁴⁸T. Janowski and P. Pulay, *Chem. Phys. Lett.* **447**, 27 (2007).
- ⁴⁹R. Knaanie, J. Šebek, J. Kalinowski, and R. B. Gerber, *Spectrochim. Acta A* **119**, 2 (2014).
- ⁵⁰M. Schütz, R. Lindh, and H.-J. Werner, *Mol. Phys.* **96**, 719 (1999).
- ⁵¹S. Carter, S. J. Culik, and J. M. Bowman, *J. Chem. Phys.* **107**, 10458 (1997).
- ⁵²G. M. Chaban, J. O. Jung, and R. B. Gerber, *J. Chem. Phys.* **111**, 1823 (1999).
- ⁵³T. K. Roy and R. B. Gerber, *Phys. Chem. Chem. Phys.* **15**, 9468 (2013).
- ⁵⁴L. Khriachtchev, A. Lignell, J. Juselius, M. Räsänen, and E. Savchenko, *J. Chem. Phys.* **122**, 014510 (2005).
- ⁵⁵See supplementary material at <http://dx.doi.org/10.1063/1.4866913> for additional tables.
- ⁵⁶A. Lignell, L. Khriachtchev, M. Räsänen, and M. Pettersson, *Chem. Phys. Lett.* **390**, 256 (2004).